NAIC-ID(RS)T-0203-95

# NATIONAL AIR INTELLIGENCE CENTER

## ALUMINUM MATRIX PARTICLE COMPOSITES AND THEIR PROPERITES

by

*Pan Ye, Gao Zhiquiang, Sun Guoxiong*



**Approved for public release: distribution unlimited.**

# HUMAN TRANSLATION

NAIC-ID (RS)T-0203-95 17 August 1995

MICROFICHE NR: 95C000505

## ALUMINUM MATRIX PARTICLE COMPOSITES AND THEIR PROPERTIES

By: Pan Ye, Gao Zhiquiang, Sun Guoxiong

English pages: 13

Source: Journal of Southeast University, Edited by the Department of Mechanical Engineering, Volume 23 Supplement, Nanjing, China, June 1993.

Country of origin: China

This document is a human translation.
Translated by: Leo Kanner Associates Redwood City, California
F33657-88-D-2188

Quality controlled by: Kristine Mastrog

Requester: NAIC/TATV R. M. Dunco
Approved for public release: distribution unlimited

GRAPHICS DISCLAIMER

All figures, graphics, tables, equations, etc. merged into this translation were extracted from the best quality copy available.

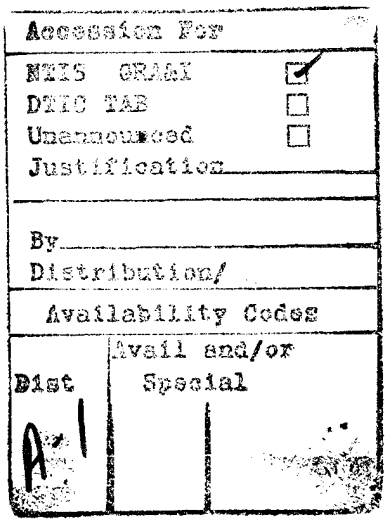

# ALUMINUM-MATRIX-PARTICLE COMPOSITES AND THEIR PROPERTIES

Pan Ye, Gao Zhiquiang, Sun Guoxiong
(Department of Mechanical Engineering)

ABSTRACT

$Al_2O_3$/ZL104 and $SiC_p$/ZL104 composites in which particles are uniformly distributed in the matrix were successfully fabricated by the liquid-solid rheological technique. Determination was made of tensile strength, wear resistance, and coefficient of thermal expansion of the composites with various particle-volume fractions. The strengthening mechanism and interface reaction between particle and matrix are also discussed.

Key words: particulate reinforced composite, aluminum alloys, properties, interface.

Using hardened particles as a strengthener for aluminum composite materials avoids the drawbacks of using fiber as a strengthener for ferrous metal-based composite materials, namely complicated processing, the high cost of fiber, and fiber losses

which are created in the manufacturing process. This also can combat the strict limitations of equilibrium phases and metastable phases imposed in growth dynamics [1], self-generated strengthening phase components, state, dimensions and relative quantity of the composite materials. Giving composite materials a very broad flexibility has recently become an important point and direction of investigation of ferrous metal-based composite materials.

This type of composite material integrates two component materials of differing physical properties and possesses a high hardness level, a low coefficient of thermal expansion, and excellent abrasion resistance and high-temperature properties [2, 3]. It also has low production costs, and, all other things being equal, can be reformed with secondary processing, so it has a broad applications future.

Because the wetting angle of ceramic particles and molten aluminum is greater than 90°, and because there is a difference in specific gravity, the strengthening matrix is easily polymerized and sunk into the aluminum-based matrix, creating an unsuitable integration interface and making the manufacture of these types of matrix composites difficult. Although powder-metallurgical methods have already been employed in the study of matrix composites to improve particle and matrix phase solubility properties, industrial use is limited due to the complexity of

powder metallurgy technology and composite processing. This article is based on float and sink resistance, and uses liquid and solid dual phase fluid methods to successfully make $Al_2O_3$/ZL104 and $SiC_p$/ZL104 matrix composites, and explores their integration capabilities.

## 1. Making Matrix Composites

ZL104 (8.85% by weight Si, 0.37% by weight Mn, 0.30% by weight Mg, Al to make up 100%) was selected as the principal alloy, and hardened ceramic $Al_2O_3$ and SiC, as the strengthening particles, with particle differentiation at 28-40μm and 40-60μm. Particles underwent appropriate heat-treatment to remove surface absorbent materials and to raise particle surface capability.

One can reduce the air absorption and oxidation of the subsequent manufacturing process by putting the ZL104 matrix alloy in a fluidized-bed device, heating to the liquid-phase temperature, putting the molten material through a deaeration process, and then, after removing the air, directing argon gas over the molten aluminum surface. During continuous cooling of the molten materials, mixing is performed by inserting an adjustable speed electric mixer, causing the alloy to cool to dual phase liquid-solid state. At this time it is in a shear-transformation liquid state, and the already-solidified dendrites splinter. We use the immiscible solid state quantity of the

liquid alloy to control viscosity. When viscosity reaches a certain value, heat-treated $Al_2O_3$ and SiC particles are added to the semi-solid state mixture at the right rate. This time, the already-solidified solid phase and the ceramic particles collide against one another, effectively reducing the ability of the particles to move, thus functioning to remove sink-resistant particles.

To ensure that the composite mixture has sufficient fluidity, we wait until the particles reach a pre-established insertion amount, and then we quickly raise the temperature to 720°C, casting a composite material.

2. Particle Distribution Uniformity

The organization of $Al_2O_{3p}$/ZL104 and $SiC_p$/ZL104 is shown in Fig. 1.

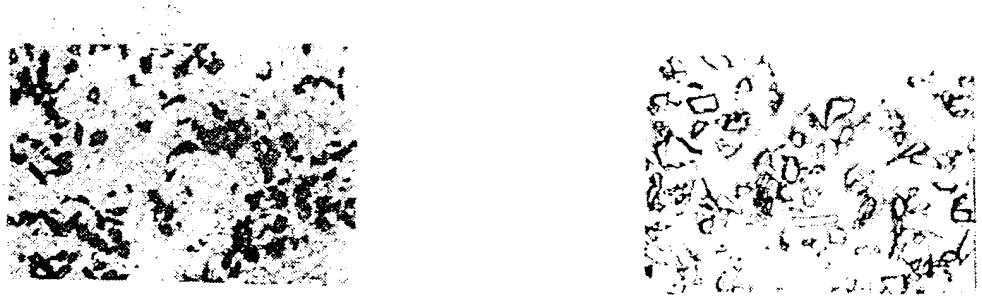

(a) $Al_2O_3$ (b) SiC

Fig. 1. Distribution of ceramic particles in base materials (magnification: 70X)

The distribution of the ceramic particles in the base materials is uniform. The interface is nonporous, and crack-free; the integration between the particles and matrix is good, without edge crystalline interface bias fusion. This type of uniform distribution is the deciding factor in obtaining high-capability composite materials.

After heating the produced $Al_2O_3$/ZL104 to 720°C, and maintaining that temperature for 30min, then melting the material three times in succession, the $Al_2O_3$ particles are still not eliminated. When heated again, the sink-resistant particles solidify to the solid phase and no longer exist. If the $Al_2O_3$ should sink, its content is greatly reduced, or uneven particle distribution results. Actually, there is still a higher uniformity and rate of collection, and the content does not change, and is stably maintained at approximately 14% by volume. This explains why the wetness of the particles and liquid aluminum is improved after entering liquid aluminum. It is not due to interface phenomenon and fusion; the existence of these scattered particles raises the apparent viscosity of the liquid aluminum and prevents the particles from being eliminated. And the cast, boss-elongated sample smoothness is complete, guaranteeing that some cast forms will have full fluidity. This special point addresses the production of composite materials, and the especially important significance of secondary forming.

## 3. Properties of Composite Materials

### 3.1. Strength Under Ambient Temperature and High Temperature

A strength test rod was maintained at 535°C for 3.5h, quenched in water at 60°C, and then at 175°C for 12h, then drawn to breaking, with the results shown in Fig. 2. $Al_2O_3p$/ZL104 and $SiC_p$/ZL104 ambient temperature strength decreases as the size and fractional number of particles decreases. Under 280°C, the strength of $Al_2O_3p$/ZL104 is still trending downward, but the rate of decrease compared to that at ambient temperature is reduced. $SiC_p$/ZL104 strength is definitely increased; when SiC size and fractional quantity is at 4% it increases by approximately 7%.

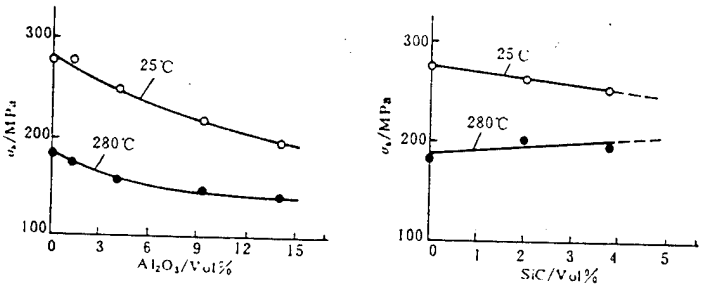


Fig. 2. Relationship between composite material strength and particle content

### 3.2 Abrasion resistance

With two types of composite materials against a grinding wheel (made of No. 45 steel with quenching and intermediate-temperature tempering), the surface line of the slide rate is

0.42m/s. When lubricated, and then abraded at 440Newtons of pressure for 2h, and then again at 880Newtons of pressure for 1h, the $Al_2O_3$ particles serve to greatly increase abrasion resistance. When particle size quantity reaches 14%, equal to the ZL104 alloy, abrasion loss was reduced by 2 scale degrees in size. The SiC particles raise abrasion resistance even more; when SiC content is only 4%, the abrasion loss was reduced by 2 scale degrees in size, as shown in Fig. 3.

Inspection of the abraded surface revealed no visible harm to the abrasion wheel, and ensured the repeatability of the experimental abrasion conditions. The ZL104-alloy abraded surface had many deep and long scars. But the abraded surface of the composite materials was relatively smooth, further proving that the hardening particles and matrix were well integrated, but not to the extent that the hardening points would fall and become abrasion scrap, creating a serious abrasion particle abrasion loss. Because SiC appears to have an apparent hardness factor (3280) higher than $Al_2O_3$ (2200-2300), its integration with the matrix is even stronger (see the detailed analysis below), so $SiC_p$/ZL104 composite materials abrasion resistance is even better.

### 3.3. Coefficient of Linear Expansion

Fig. 4 shows the relationship between average linear

coefficient of expansion and particle size and quantity for the two types of composite materials in the range of 35-329°C. From this figure, one can see that, with the addition of the particles, only the linear expansion coefficient decreases, and when particle size and quantity are 14%, it decreases 30%. This symbolizes the great advantage of using compatible low linear expansion coefficient composite materials.

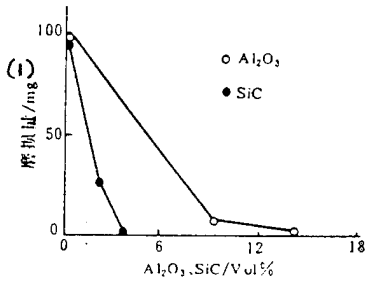


Fig. 3. Effect of particle content on abrasion resistance
KEY: 1. (x-axis:) quantity abraded/mg

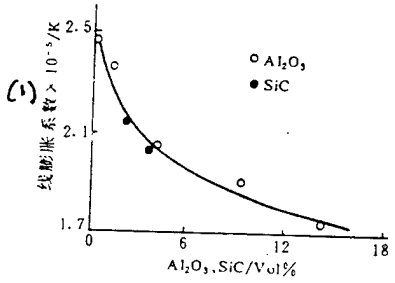


Fig. 4. Effect of particle content on linear expansion coefficient
KEY: 1. (x-axis:) linear expansion coefficient

## 4. Discussion

For particle-hardened materials, load bearing relies primarily on the matrix material, and its strength derives from

the ability of the scattered particles to resist dislocation of the matrix. According to the Orowan Strengthening Mechanism, strengthening should be based on the relationship between $\Delta\tau$ and particle size and quantity $V_p$, as shown in the following formula [8]:

$$\Delta\tau = \frac{\sqrt{3}}{(2\pi)^{3/2} \cdot K} \cdot \frac{G \cdot b \cdot V_p^{1/2}}{r} \cdot \ln \frac{d}{r_0} \qquad (1)$$

In the equation, G is the shear conversion of the matrix material, b is dislocation, b is Burger's dislocation vector, d is average distance between the particles, r is particle diameter, $r_0$ is the diameter of Hooke's law-based efficiency loss; K is a dislocation-type indicator (for a screw-type dislocation, K=1, for a blade-type dislocation, K=2/3).

Eq. (1) shows that materials strength increases with an increase in $V_p$. Clearly, this scheme is not suitable for acicular particles with a diameter of 28-60μm (see Fig. 1). This is because the dispersed particles in the strengthened materials form balls, generally measuring 0.1-2μm in size, and particle distance is less than 5μm, effectively eliminating dislocation. If particle distance in composite materials is too large, one cannot rely on the particle-distance-dislocation curve to bring about strengthening. In addition, acicular particles can create serious stress points and weaken the matrix.

Although we have researched formulas [7] for expressing the

strength of particle composite materials, the results are closer to practice than the results from Eq. (1). Because we have not entered the area of interface integration strengthening, we are unable to fully disclose the laws of strengthening of the composite materials. It is not easy to test interface integration strengthening, making it difficult to construction a method of expressing it. We have now discovered a close relationship between maximum elongation $\delta_0$ while breaking, and interface integration strength. When interface integration strength is high, creation of tiny fissures in the matrix due to interface openings is less likely. And macroscopic performance, expressed as $\delta_0$, increases. This provides the possibility of a method of expressing an interface-integration-strength reference number. This research is currently underway.

Fractographic analysis shows a large quantity of hard apertures existing in the matrix, and fissure cracks on the sharp ends of some particles. As one can see, concentrated stress points promote the formation and expansion of cracks. The tight integration of particles and the matrix, without separation (see Fig. 5), indicates good integration of particles and the matrix. The surface smoothness of $Al_2O_3$ particles, free of the scars of the matrix materials (see Fig. 5(a), (b)), does not reflect the existence of an interface. Levi believes [8] that $Al_2O_3$ and the Mg in molten alloy reflects the generation of an $MgAl_2O_4$ interface layer: $4Al_2O_3+3Mg->3MgAl_2O_4+2Al$. After calculation,

this reflects that at a standard of below 993K, the free-enthalpy change $\Delta G^\circ$= -244kJ, satisfying the thermodynamic conditions. But this research uses a very low Mg-content-matrix alloy, of only 0.30% by weight, actually subject to the limitations of reaction dynamics, and an interface layer is not easily generated. When the quantity of Mg added surpasses 1% by weight, an $MgAl_2O_4$ interface layer exists. This interface layer can raise the integration strength of the particles and the aluminum matrix.

(a) $Al_2O_3$ 400× (b) $Al_2O_3$ 1000× (c) SiC 1000×

Fig. 5. Appearance of fractures in composite materials

A small quantity of matrix materials adheres to the SiC particles (Fig. 5 (c)), demonstrating a fairly good metallurgical integration between SiC and the matrix. Is this caused by the generation of the $Al_4C_3$ interface layer? Calculations reflect that the standard-free-enthalpy change of $4Al+3SiC \rightarrow Al_4C_3+3Si$ [10] results in $\Delta G^\circ$=203KJ under 993K, and that SiC cannot react with Al to form $Al_4C_3$. But without the existence of the lubricating center layer between the particles and matrix, it is

very difficult to have the integration strength of the particle surfaces adhering to the matrix. This may be because the free carbon in SiC and Al react to form an interface layer: 3C (graphite) +4Al-> $Al_4C_3$. In this reaction, $\Delta G^\circ$= -113kJ. $Al_4C_3$ is very brittle, and unstable under some conditions, but it can reasonably control the quantity formed, and is definitely advantageous to improving the lubrication conditions of the interface.

## 5. Conclusions

a. Using liquid- and solid-phase rheological methods can successfully produce non-packaged $Al_2O_3$ and SiC particle aluminum based composite materials, with uniform particle distribution and good interface integration. Especially after multiple melting, the $Al_2O_3$ particle content can be stably maintained at primary levels.

b. $Al_2O_3$/ZL104 and $SiC_p$/ZL104 ambient temperature strength $\sigma_b$ decreases with increases in $V_p$. This is related to particle size, larger particle distance, and sharp corners. However, when Al2O3 content reaches 14% by volume, $\sigma_b$ can reach 19.6MPa; when SiC content is 0.4% by volume, $\sigma_b$ can reach 25.5MPa. Below 280°C, $Al_2O_{3p}$/ZL104 $\sigma_b$ shows an obvious and dramatic decrease with an increase in $V_p$, and $SiC_p$/ZL104 $\sigma_b$ is increased substantially.

c. In comparison to matrix alloys with ZL104, the abrasion resistance of the two components in the composite material is greatly increased, and the linear expansion coefficient is obviously decreased. We hope that these will become lightweight, inexpensive, precision, high temperature-resistant materials.

REFERENCES


1 Rohatgi P K, et al. Int Met Rev, 1986; 31:115

2 Surappa M K, et al. J Mat Sci, 1981;16:983

3 Deonath R N, et al. J Mat Sci, 1981; 16:3025

4 Lewandowski J J, et al. Processing and Properties for Powder Metallurgy Composites. The Metallurgical Society, Inc, 1988; 117

5 曹 阳等. 复合材料学报,1992; 9(3): 33

6 费豪文 J D. 物理冶金学基础. 上海科学技术出版社,1981;244

7 Majumdar S S, et al. Mater Sci Eng, 1984;68:85

8 Levi C G, et al. Met Trans, 1978;9A:697

9 唐 力. 南京工学院硕士论文,1987

10 Moshier W C, et al. J Mat Sci, 1987; 22:1154

# DISTRIBUTION LIST

## DISTRIBUTION DIRECT TO RECIPIENT

| ORGANIZATION | MICROFICHE |
|---|---|
| B085 DIA/RTS-2FI | 1 |
| C509 BALLOC509 BALLISTIC RES LAB | 1 |
| C510 R&T LABS/AVEADCOM | 1 |
| C513 ARRADCOM | 1 |
| C535 AVRADCOM/TSARCOM | 1 |
| C539 TRASANA | 1 |
| Q592 FSTC | 4 |
| Q619 MSIC REDSTONE | 1 |
| Q008 NTIC | 1 |
| Q043 AFMIC-IS | 1 |
| E404 AEDC/DOF | 1 |
| E410 AFDTC/IN | 1 |
| E429 SD/IND | 1 |
| P005 DOE/ISA/DDI | 1 |
| 1051 AFIT/LDE | 1 |
| P090 NSA/CDB | 1 |

Microfiche Nbr: FTD95C000505
NAIC-ID(RS)T-0203-95